



Molecular cloning, structure, and reactivity of the second bromoperoxidase from *Ascophyllum nodosum* ☆,☆☆

Diana Wischang^a, Madlen Radlow^a, Heiko Schulz^a, Hans Vilter^b, Lutz Viehweger^c, Matthias O. Altmeyer^{d,1}, Carsten Kögler^d, Jennifer Herrmann^d, Rolf Müller^d, Fanny Gaillard^{e,f}, Ludovic Delage^{g,h}, Catherine Leblanc^{g,h}, Jens Hartung^{a,*}

^aFachbereich Chemie, Organische Chemie, Technische Universität Kaiserslautern, Erwin-Schrödinger-Straße, D-67663 Kaiserslautern, Germany

^bZurmaiener Straße 16, D-54292 Trier, Germany

^cLandesamt für Verbraucherschutz Sachsen-Anhalt, Fachbereich 3 Lebensmittelsicherheit, Postfach 200857, D-06009 Halle (Saale), Germany

^dHelmholtz-Institut für Pharmazeutische Forschung, Helmholtz-Zentrum für Infektionsforschung und Pharmazeutische Biotechnologie, Universität des Saarlandes, Campus, D-66123 Saarbrücken, Germany

^eUPMC Université Paris 6, FR 2424, Station Biologique, F-29680 Roscoff, France

^fCNRS, FR 2424, Station Biologique, F-29680 Roscoff, France

^gUPMC Université Paris 6, UMR 7139 Végétaux marins et Biomolécules, Station Biologique, F-29680 Roscoff, France

^hCNRS, UMR 7139 Végétaux marins et Biomolécules, Station Biologique, F-29680 Roscoff, France

ARTICLE INFO

Article history:

Received 2 March 2012

Available online 23 June 2012

Keywords:

Ascophyllum nodosum

Bromoperoxidase

Fucales

Kinetics

Linear free energy relationship

Organobromine synthesis

Oxidation catalysis

Phenol bromination

Vanadium

ABSTRACT

The sequence of bromoperoxidase II from the brown alga *Ascophyllum nodosum* was determined from a full length cloned cDNA, obtained from a tandem mass spectrometry RT-PCR-approach. The clone encodes a protein composed of 641 amino-acids, which provides a mature 67.4 kDa-bromoperoxidase II-protein (620 amino-acids). Based on 43% sequence homology with the previously characterized bromoperoxidase I from *A. nodosum*, a tertiary structure was modeled for the bromoperoxidase II. The structural model was refined on the basis of results from gel filtration and vanadate-binding studies, showing that the bromoperoxidase II is a hexameric metalloprotein, which binds 0.5 equivalents of vanadate as cofactor per 67.4 kDa-subunit, for catalyzing oxidation of bromide by hydrogen peroxide in a bi-bi-ping-pong mechanism ($k_{\text{cat}} = 153 \text{ s}^{-1}$, 22 °C, pH 5.9). Bromide thereby is converted into a bromoelectrophile of reactivity similar to molecular bromine, based on competition kinetic data on phenol bromination and correlation analysis. Reactivity provided by the bromoperoxidase II mimics biosynthesis of methyl 4-bromopyrrole-2-carboxylate, a natural product isolated from the marine sponge *Axinella tenuidigitata*.

© 2012 Elsevier Inc. All rights reserved.

Abbreviations: BCD, 2-bromo-2-chlorodimedone; cDNA, complementary DNA; HEPES, 4-(2-hydroxyethyl)-1-piperazinethanesulfonic acid; ICP, inductively coupled plasma; MES, 2-(4-morpholino)ethanesulfonic acid; Tris, tris-(hydroxymethyl)-aminomethane; U, amount of enzyme required for turning over 1 μmol of substrate per minute; U_T, peroxidase activity determined in the triiodide (T)-assay; U_{MCD}, bromoperoxidase activity determined in the monochlorodimedone (MCD)-assay; U_T, bromoperoxidase activity determined with the aid of the triiodide assay (T); U_T⁰ mg⁻¹, specific bromoperoxidase activity in units per mg of enzyme at the beginning of a reaction, specific activity referring to the number of units per mg of enzyme; V_{Br}PO, vanadate(V)-dependent bromoperoxidase; *An*, *Ascophyllum nodosum*; V_{Br}PO(*An*I), V_{Br}PO-isoenzyme I from *Ascophyllum nodosum*; V_{Br}PO(*An*II), V_{Br}PO-isoenzyme II from *A. nodosum*; V_{Br}PO(*Fd*), V_{Br}PO from *Fucus distichus*; V_{Br}PO(*Ld*I), V_{Br}PO-isoenzyme I from *Laminaria digitata*.

* This work was supported by the Deutsche Bundesstiftung Umwelt (Grant 20008/982; scholarship for D.W.), the Stiftung für Innovation des Landes Rheinland-Pfalz (Grant No. 818), and NanoKat.

☆☆ The nucleotide sequence reported in this paper has been submitted to the EBI Data Bank with accession no. HE598751.

* Corresponding author. Fax: +49 631 205 3921.

E-mail address: hartung@chemie.uni-kl.de (J. Hartung).

¹ Present address: KIST Europe Forschungsgesellschaft mbH, Universität Saarbrücken, Campus E7.1, D-66123 Saarbrücken, Germany.

1. Introduction

From organic matter preserved in lithospheric sediments and crustal ice [1], scientists have concluded that organobromines are, and probably always have been, an integral part of a planetary cycle that transports bromide from ocean water via secondary metabolites [2–4] and volatile organic compounds [5,6] to mineral deposits or continental brines [7,8].

The common structural motif of naturally occurring organobromines is the covalent carbon-bromine bond, which is formed in the marine environment via nucleophilic substitution, homolytic displacement by radical intermediates, or electrophilic addition [9]. Whereas free radical reactions dominate for hydrocarbon bromofunctionalization in the marine boundary layer, electrophilic bromination of carbon nucleophiles explains the majority of secondary metabolite formation in marine organisms, on the basis of common mechanistic sense [7,10–12].

The electron acceptor to convert bromide into a bromoelectrophile in the majority of organisms is hydrogen peroxide, which is

biosynthetically produced, for example, from glucose oxidase-catalyzed dioxygen reduction [13]. Oxidation of bromide by hydrogen peroxide in neutral to weakly acidic aqueous solution, however, is slow and requires catalysis to successfully compete with other hydrogen peroxide-consuming processes [14]. In order to accelerate the rate of bromide oxidation by hydrogen peroxide, marine organisms have developed enzymes, such as the vanadate-dependent bromoperoxidases ($V_{Br}PO$) [15–18].

Vanadate is a transition metal that shares many chemical characteristics with phosphate. At the activity maximum of marine bromoperoxidases (pH 6–7), vanadate exists in millimolar solution as dihydrogenvanadate ($H_2VO_4^-$), the conjugated base of orthovanadic acid H_3VO_4 ($pK_a^1 = 3.5$, $pK_a^2 = 7.8$, $pK_a^3 = 12.5$). Dihydrogenvanadate shows strong affinity for binding to bromoperoxidase proteins at the τ (*tele*, remote) imidazole nitrogen of a histidine side chain, to provide an active site for bromide oxidation [19–21]. The vanadate cofactor and proximate amino acid side chains thereby provide a template for locking water molecules into a supramolecular network, to facilitate hydrogen peroxide binding and subsequent bromide oxidation [20].

From a chemical point of view, bromide oxidation mediated by peroxides at pH 6–7 furnishes hypobromous acid (HOBr). In an aqueous solution of bromide, such as ocean water, hypobromous acid furnishes an equilibrium mixture of HOBr, molecular bromine, and tribromide [19,20]. According to the general mechanistic scheme for bromoperoxidase-catalyzed oxidation, carbon–bromine bond formation occurs in a non enzymatic reaction between an organic acceptor and HOBr, Br_2 , or Br_3^- [14]. Bromoperoxidases therefore show little to no organic substrate specificity.

A rewarding source for isolating vanadate(V)-dependent bromoperoxidases ($V_{Br}POs$) is the brown alga *Ascophyllum nodosum* (*An*) [22,23] that grows abundantly along North Atlantic shore lines [24]. The bromoperoxidase I of this alga [$V_{Br}PO(AnI)$] was the first marine bromoperoxidase to be discovered [22,25,26], and has over the years been studied in detail concerning structure [19,27], kinetics of bromide oxidation [28], (pseudo)halide-selectivity [29,30], immobilization onto magnetic beads [31], and use for synthesis of organobromines from hydrocarbons, hydrogen peroxide, and ocean water [14,32].

To supplement the pattern of bromoperoxidase reactivity and selectivity for synthesis of organobromines [20], we turned our attention in this study to a second bromoperoxidase (isoenzyme II) which is located on the thallus surface [33,34] of *A. nodosum*. We purified this enzyme in larger quantity and determined its structure via (i) molecular cloning of a full length cDNA, (ii) amino acid-sequence analysis (primary structure), (iii) CD-spectroscopy (secondary structure), (iv) modeling of the three-dimensional structure, and (v) gel filtration (quaternary structure). We furthermore measured kinetics of bromide oxidation and explored mechanistic and synthetic aspects of (het)arene bromination. The most important findings from this study show that the bromoperoxidase II from *A. nodosum* is a hexameric metalloprotein, which binds 0.5 equivalents of vanadate per 67.4 kDa-protein subunit (mass estimated from the putative mature protein composed of 620 amino acids). Vanadate is the cofactor for hydrogen peroxide activation and bromide oxidation in a bi-bi-ping-pong mechanism, to provide a bromoelectrophile showing similar reactivity in arene bromination, as molecular bromine. To exemplify that reactivity of the bromoperoxidase II mimics biosynthesis of naturally occurring organobromines, we prepared in an enzymatic approach methyl 4-bromopyrrole-2-carboxylate, a natural product isolated from the marine sponge *Axinella tenuidigitata* [35].

2. Materials and methods

2.1. cDNA cloning and sequencing

A. nodosum thalli were collected from the rocky shore in the vicinity of Roscoff (Brittany, France), and immediately frozen in liquid nitrogen. Total RNA was extracted according to Apt et al. [36] and quantified by Nanodrop ND 1000 spectrophotometer (Labtech International LTD., East Sussex, UK). Total RNA was used as a template for reverse transcription followed by a polymerase chain reaction (RT-PCR) to amplify a cDNA fragment using degenerate primers designed from LC-MS/MS data. The 5' and 3' end part of the cDNA sequence were then obtained using rapid amplification of cDNA ends (RACE) approaches. The 3' end sequence was cloned using the protocol developed by Scotto-Lavino et al. [37] and the 5' end part using the SMART RACE cDNA amplification kit (Clontech) according to the manufacturer's recommendations. Using two specific primers, the full length cDNA was then amplified by PCR, cloned into the pCR 2.1-TOPO vector (Invitrogen) and fully sequenced on both strands using the ABI prism 3100 genetic analyzer (Applied Biosystems).

2.2. Bromoperoxidase preparation for steady-state kinetics and reactivity studies

$V_{Br}PO(AnII)$ was isolated from *A. nodosum* collected in April 2009 in close proximity to the Station Biologique Roscoff/Brittany (France, 48°43'N, 3°58'W). A fraction containing bromoperoxidase isoenzymes was obtained from freeze-dried algae according to an improved liquid–liquid–partitioning process [26]. The crude solution was enriched with a $(NH_4)_2SO_4$ step gradient (15% → 0%) using Phenyl Sepharose™ 6 FF as stationary phase. After pooling the two relevant fractions accumulated with $V_{Br}PO(AnI)$ and $V_{Br}PO(AnII)$, the enzymes were furthermore concentrated by hydrophobic interaction chromatography (HIC) using a $(NH_4)_2SO_4$ linear gradient (15% → 0%). $(NH_4)_2SO_4$ weight percent was pursued by conductivity measurement. The characteristic band at 280 nm was used for detection of bromoperoxidases. $V_{Br}PO(AnI)$ was purified to homogeneity by gel filtration [size exclusion chromatography (SEC), Sephacryl™ S-300 HR] from the first HIC-fraction (Fig. 1, left). $V_{Br}PO(AnII)$ was purified to homogeneity by gel filtration from the second HIC-fraction (Fig. 1, center).

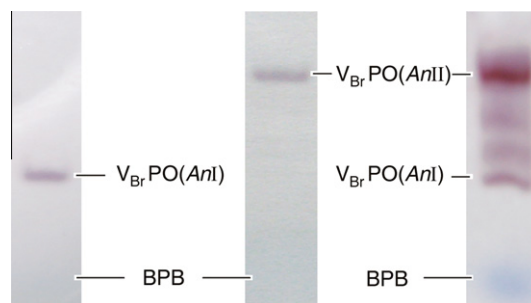


Fig. 1. Polyacrylamide gel electrophoresis (1 h, 18 mA; non-denaturing conditions) of bromoperoxidase fraction obtained from liquid–liquid partitioning processes and FPLC (right), purified [hydrophobic interaction chromatography (HIC) and size exclusion chromatography (SEC)] bromoperoxidases $V_{Br}PO(AnII)$ (center, BPB = bromophenol blue), and $V_{Br}PO(AnI)$ (left). All lanes: 5 μ L from a solution of 80 μ L dialyzed extract (see Materials and Methods), 20 μ L H_2O (bidest.), saccharose (40 mg) and a solution of BPB in [0.1% (w/w) in H_2O (bidest.)]. Staining was performed in a solution prepared from phosphate buffer (100 mL), H_2O_2 (10 mL), aq. KI (100 μ L) (for concentrations of the three reagents, see triiodide test), and 1,4-phenyldiammonium dichloride (100 mg) [26].

2.3. Molecular mass determination

Bromoperoxidase II was obtained as approximately 200 $\mu\text{g}/\text{mL}$ solution in 50 mM Tris/HCl buffer. Reference proteins (Gel Filtration Standard, BioRad) were dissolved in 10 mM sodium acetate buffer containing 250 mM NaCl (pH 4.75), which also served as the mobile phase. Proteins were separated with a flow rate of 1 mL/min using a BioSep-SEC-S column (600 mm \times 7.8 mm; Phenomenex). Molecular masses of bromoperoxidases were determined based on linear regression of retention times and common logarithms of molecular masses of the reference proteins.

2.4. Steady-state kinetics

Specific activity of $V_{\text{Br}}\text{PO}(\text{AnII})$ used for steady-state kinetic experiments was $87 \pm 4 \text{ U}_{\text{MCD}}^0 \text{ mg}^{-1}$ (MCD-assay) [38] and $565 \pm 5 \text{ U}_{\text{T}}^0 \text{ mg}^{-1}$, respectively (triiodide assay; see the [Supplementary Material](#)). MCD-bromination for kinetic studies was performed in MES buffered solution (50 mM, pH 5.9) or HEPES-buffered solution (50 mM, pH 7.2) containing 1 mM–400 mM of KBr. The ionic strengths was adjusted to $I = 0.8 \text{ M}$ with Na_2SO_4 . The H_2O_2 concentration was varied from 0.02 mM to 1 mM. $V_{\text{Br}}\text{PO}(\text{AnII})$ ($M = 134\,929 \text{ Da}$ for the vanadate-loaded dimer, which is the smallest unit carrying one active site) was used from a 1.4 μM stock solution in Tris/HCl buffer (50 mM) with the added volumes ranging from 10 and 40 μL , depending on the total rate of bromide oxidation. All measurements were performed at $22.0 \pm 0.5 \text{ }^\circ\text{C}$. The initial rates, v , as a function of H_2O_2 or Br^- concentration were fitted according to the Michaelis–Menten relationship, that is $v = V[\text{H}_2\text{O}_2]/(K + [\text{H}_2\text{O}_2])$, where V and K are functions of $K_{\text{m}}^{\text{Br}^-}$, $K_{\text{m}}^{\text{H}_2\text{O}_2}$, V_{max} , $K_{\text{i}}^{\text{Br}^-}$ at substrate saturation concentration (see the [Supplementary Material](#)) [14,28].

2.5. General method for competition kinetics

In three independent runs, a stock solution A [3.75 mL, corresponding to 20 μmol of NaBr], consisting of MES-buffer (50 mM, pH 6.2, 225 mL) and NaBr (124 mg, 1.20 mmol), was added to a mixture of phenol (**1a**) and 2-substituted derivatives **1b–1e** in ratios of 1:1, 1:2, and 2:1 (200 μmol or 400 μmol). To this mixture, MES-buffer (50 mM, pH 6.2, 3.75 mL), *t*BuOH (2.5 mL) and $V_{\text{Br}}\text{PO}(\text{AnII})$ [61.9 μL (0.1130 mg/mL; 572 $\text{U}_{\text{T}}/\text{mg}$), 4.0 U_{T} , 0.27 mmol% referenced toward the vanadate-loaded dimer] was added. The resulting reaction mixture was treated with H_2O_2 (2 mL, 10 mM) in a dropwise manner within 2 min, and stirred at 25 $^\circ\text{C}$ for 24 h. Afterwards, the pH of the mixture was adjusted with 2 M aq. HCl to 1 and the organic products were extracted with Et_2O (2 \times 15 mL, 1 \times 10 mL). Combined organic extracts were dried (MgSO_4) and concentrated under reduced pressure (13 mbar, 40 $^\circ\text{C}$). The residue was treated with a stock solution B (0.3 mL), consisting of $\text{Zn}(\text{ClO}_4)_2 \times 6 \text{ H}_2\text{O}$ (60.0 mg, 0.16 mmol) in Ac_2O (1.10 g, 10.8 mmol) and Et_2O (0.9 mL), stirred for 18 h at 25 $^\circ\text{C}$, subjected to adsorptive filtration (SiO_2 , EtOAc), and analyzed by GC using *n*-decane as an internal standard.

2.6. Bromination of methyl pyrrole-2-carboxylate

A solution of H_2O_2 (2.0 mL, 0.825 M) and NaBr (170 mg, 1.65 mmol) in MES-buffer (500 mM, pH 6.2) was added with a syringe pump (20 h, 1.67 $\mu\text{L}/\text{min}$) to a solution of substrate **4** (0.75 mmol) and $V_{\text{Br}}\text{PO}(\text{AnII})$ (546 μL , 34.6 U_{T} , 63 $\mu\text{mol}\%$) in MES-buffer (500 mM, pH 6.2, 10.0 mL) and *t*BuOH (3.3 mL). The reaction mixture was stirred at 23 $^\circ\text{C}$ for 24 h. The aqueous layer was extracted with Et_2O (4 \times 10 mL). Combined organic extracts were dried (MgSO_4). The solvent was removed under reduced pressure (40 mbar, 40 $^\circ\text{C}$) to afford a product mixture which was analyzed

by ^1H NMR (pentachlorobenzene as internal standard) and GC ([Supplementary Material](#)). Final pH and bromoperoxidase activity (triiodide assay) were determined from the aqueous layer.

3. Results and discussion

3.1. Structure of bromoperoxidase II from *A. nodosum*

3.1.1. Purification and primary structure

A. nodosum (*An*) was freeze-dried, milled, and subjected to a liquid–liquid partitioning process [25,26] to afford by acetone-precipitation a colorless powder of crude bromoperoxidases. The powder was dissolved in tris-(hydroxymethyl)-aminomethane (Tris)/hydrochloric acid (HCl)-buffer (pH 9.0) and dialyzed against sodium metavanadate, showing in colorless native (CN) polyacrylamide gel electrophoresis (PAGE) upon staining at least five spots of bromoperoxidase activity (Fig. 1, right). From this mixture, $V_{\text{Br}}\text{PO}(\text{AnI})$ (Fig. 1, left) and isoenzyme II [$V_{\text{Br}}\text{PO}(\text{AnII})$] (Fig. 1, center) were separated via hydrophobic interaction chromatography and size exclusion chromatography, to afford solutions containing up to 180 $\mu\text{g mL}^{-1}$ of the bromoperoxidases. The identity of $V_{\text{Br}}\text{PO}(\text{AnI})$ was determined via MALDI-ToF analysis of trypsin-digested samples, and data base analysis of measured tryptic peptide masses in comparison to the known primary structure of the enzyme (PDB 1QI9) [19].

To measure bromoperoxidase activity of isoenzyme II, we used the triiodide assay (U_{T}^0) [39,40]. In this photometric test, triiodide ($\lambda_{\text{max}} = 350 \text{ nm}$) is formed from iodide and hydrogen peroxide. The rate of enzyme-catalyzed triiodide formation thereby is corrected for the uncatalyzed reaction between hydrogen peroxide and iodide, using a double beam spectrometer. According to this assay, the activity of the purest samples, which we used for conducting steady-state kinetics, ranged between 889 and 565 $\text{U}_{\text{T}}^0 \text{ mg}^{-1}$ (phosphate buffer, pH 6.2). Samples showing activity between 572 and 380 $\text{U}_{\text{T}}^0 \text{ mg}^{-1}$ were used for mechanistic and synthetic studies summarized in Section 3.2. In Tris/HCl-buffer (pH 9) the bromoperoxidase II retained full enzymatic activity, if stored at 4 $^\circ\text{C}$ (checked for three months; [Supplementary Material](#)).

Since other research groups customarily determine bromoperoxidase activity by the monochlorodimedone (2-chlorodimedone or MCD)-assay [38,39,41], we performed this test in addition, to reference our data from the triiodide assay. In the MCD-assay, a time dependent decrease of the MCD-absorbance at $\lambda_{\text{max}} = 290 \text{ nm}$ [$\epsilon_{290} = 2010 \text{ m}^2 \text{ mol}^{-1}$] is correlated with 2-bromo-2-chlorodimedone (BCD)-formation [$\epsilon_{290} = 20 \text{ m}^2 \text{ mol}^{-1}$] [42] via electrophilic bromination [32]. In the MCD-test, the activity of the purest $V_{\text{Br}}\text{PO}(\text{AnII})$ -samples was 87–117 $\text{U}_{\text{MCD}}^0 \text{ mg}^{-1}$ (pH 6.5, phosphate buffer), which compares to the activity of isoenzyme I (127 to 171 $\text{U}_{\text{MCD}}^0 \text{ mg}^{-1}$), but is by a factor 10 smaller than activity of bromoperoxidases isolated from *Macrocystis pyrifera* (1730 $\text{U}_{\text{MCD}}^0 \text{ mg}^{-1}$) and *Fucus distichus* (1580 $\text{U}_{\text{MCD}}^0 \text{ mg}^{-1}$) [13]. The origin of this difference by one order of magnitude in activity between bromoperoxidases from the latter two organisms and *A. nodosum* is not yet known.

For primary structure analysis of $V_{\text{Br}}\text{PO}(\text{AnII})$, we cloned a full length cDNA from *A. nodosum*, based on both tandem mass spectrometry data of purified $V_{\text{Br}}\text{PO}(\text{AnII})$ and RT-PCR approaches. The cloned bromoperoxidase cDNA [2261 base pairs (bp)] features a short 5'UTR (38 bp) and a larger 3'UTR (297 bp), and encodes a protein composed of 641 amino acids. The molecular mass of $V_{\text{Br}}\text{PO}(\text{AnII})$ was determined by mass spectrometric analysis of purified excised bands from SDS–PAGE gels (see [Supplementary Material](#)), digested by trypsin. Nano-LC-MS/MS analysis showed up to 23 peptides with full or partial *de novo* sequence identity with peptides of the translated cDNA, homogeneously covering 50% of putative mature bromoperoxidase II (Fig. 2). From this

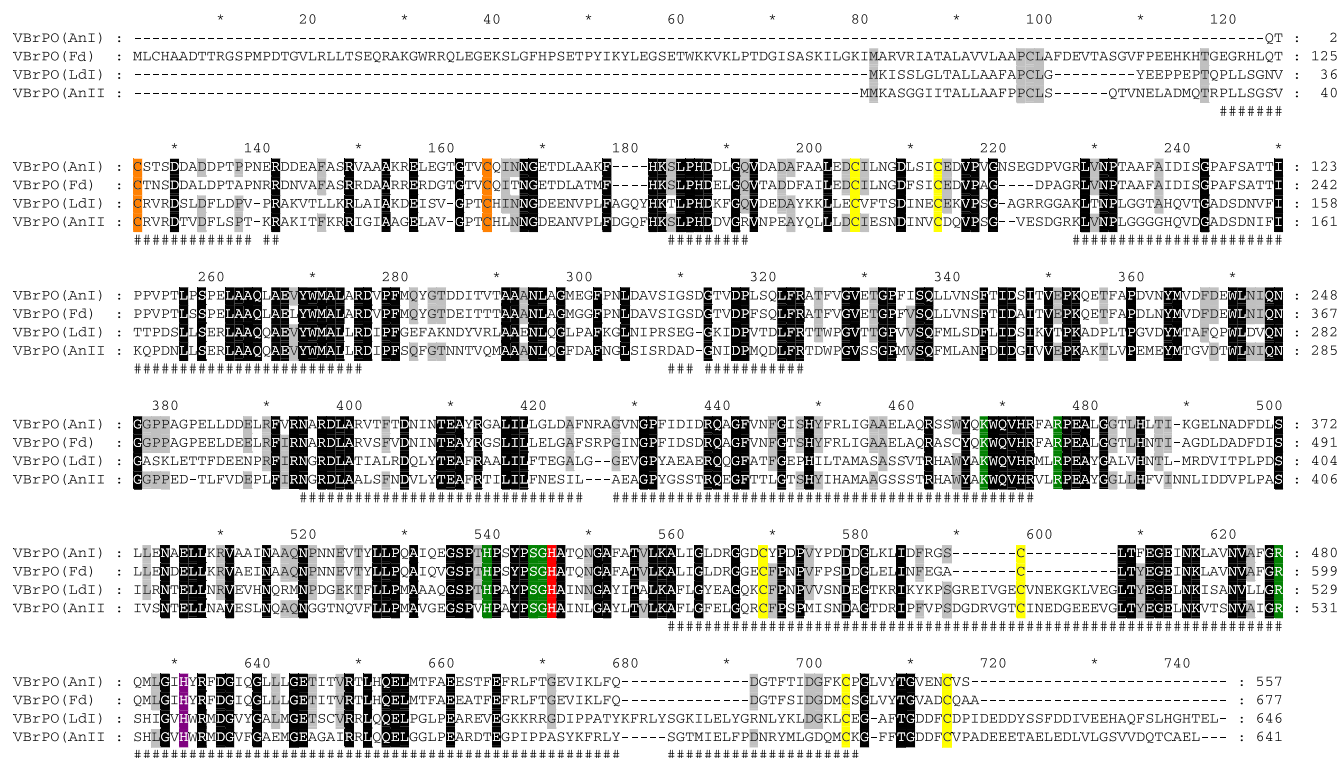


Fig. 2. Amino acid sequence alignment of $V_{Br}PO$ s from brown algae [for $V_{Br}PO(AnI)$ see No. P81701 in UniProt database, for $V_{Br}PO(Fd)$ No. O82433, for $V_{Br}PO(LdI)$ No. Q7X9V1, for $V_{Br}PO(AnII)$ No. EMBL accession No. HE598751]. Conserved residues in all proteins are shown in white capitals on black background, and the residues that occur in at least three of the sequences are in black capitals on gray background. Amino acid residues associated with the catalytic site in the $V_{Br}PO(AnI)$ three dimensional structure [19], conserved in the given proteins are colored in red (catalytic histidine), purple (vanadium binding site), and green (residues associated with the active site). Cysteine residues involved in disulfide bridging are colored in orange (intermolecular bridge) and in yellow (intramolecular). Peptides identified by LC-MS/MS analysis from purified $V_{Br}PO(AnII)$ are indicated by # below the alignment.

information we concluded that the cloned cDNA encodes the bromoperoxidase II-protein. A signal peptide was predicted with a cleavage site after the Ser-21 residue. Based on the amino acid composition of the putative mature protein, we derived a molecular mass of 67439 Da for the $V_{Br}PO(AnII)$ -protein. The *in silico* prediction of an apoplasmic location is in agreement with a previous first description of the bromoperoxidase located at the thallus surface of *A. nodosum* [34].

The $V_{Br}PO(AnII)$ -protein sequence features amino-acid residues that are conserved in other $V_{Br}PO$ s, such as the site of vanadate cofactor binding in $V_{Br}PO(AnI)$ [19] (Fig. 2). Compared to other $V_{Br}PO$ s from *Fucales*, the $V_{Br}PO(AnII)$ protein sequence exhibits 43% identity with $V_{Br}PO(AnI)$ and 42% with $V_{Br}PO(Fd)$ (from *Fucus distichus*). The $V_{Br}PO(AnII)$ -sequence is surprisingly closer to $V_{Br}PO(LdI)$ (from *Laminaria digitata*) than $V_{Br}PO(AnI)$, showing 61% amino-acid identity with the former. $V_{Br}PO(LdI)$ and $V_{Br}PO(AnII)$ furthermore share amino-acid insertions of similar lengths at the C-terminus (Fig. 2), suggesting common origin, possibly by $V_{Br}PO$ -gene duplication in an ancestor brown alga.

3.1.2. Vanadate-binding to the apoenzyme

Vanadate is an essential cofactor for catalyzing bromide oxidation by hydrogen peroxide by $V_{Br}PO(AnII)$, as determined in a dialysis-reconstitution study. Dialysis of catalytically active bromoperoxidase II in a solution of Tris/HCl-buffer versus an aqueous solution of ethylenediaminetetraacetate (EDTA) [22], lowered peroxidase activity from $326 \pm 15 U_T mg^{-1}$ to $10 \pm 1 U_T mg^{-1}$. The solution of apobromoperoxidase II then was treated at 20 °C with 0.64 μM aqueous sodium orthovanadate (pH 9.0), leading to progressive recovery of peroxidase activity to about 90% of the original value in a rapid first phase, while the remaining 10% of peroxidase

activity recovered in a second slower phase. The final activity of $370 \pm 19 U_T mg^{-1}$ after 5 h of incubation is almost identical to the original enzyme activity (Fig. 3). A fit of the time dependence increase of bromoperoxidase II-activity by a second order exponential function ($r = 0.994$) gave a half-reconstitution time of 2.2 min, which is by a factor 23 shorter than the reconstitution rate for apobromoperoxidase I under identical conditions (Supplementary Material).

The ratio of vanadate cofactor per monomeric subunit in active bromoperoxidase II was derived from quantitative vanadium analysis by inductively coupled plasma mass spectrometry (ICP-MS), starting with $V_{Br}PO(AnI)$ to reference the method. In order to secure that only enzyme-bound vanadate(V) is detected by vana-

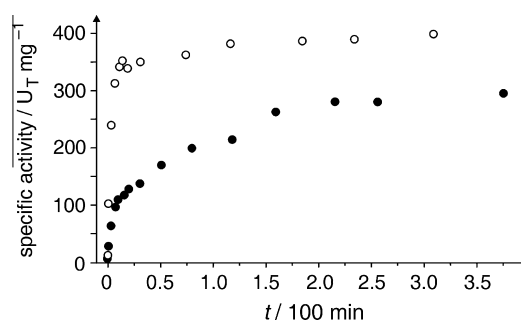


Fig. 3. Time-dependency of peroxidase activity reconstitution from dialyzed metalloenzymes $apo-BrPO(AnI)$ (●) and $apo-BrPO(AnII)$ (○) (in Tris/HCl buffer, pH 9.0, 25 mM; $T = 23$ °C) and Na_3VO_4 -solutions [for $apo-BrPO(AnI)$ 0.70 μM ($M = 60$ 189 Da) and for $apo-BrPO(AnII)$ 0.32 μM ($M = 134$ 878 Da for the smallest entity binding one vanadate cofactor)].

dium analysis, protein solutions were filtrated through a membrane having a 10 kDa-cutoff, for removing externally bound vanadate. Likewise obtained solutions of known bromoperoxidase concentration then were mineralized in a microwave pressure autoclave by dissolving the enzyme in ultra-clean nitric acid and hydrogen peroxide [26]. We furthermore measured chloride concentration of the analytes prior to ICP-MS analysis. A concentration of 4.89 mM of chloride for solutions of both bromoperoxidases was below the critical value that would have given rise to interfering signals from $^{35}\text{Cl}^{16}\text{O}^+$ in the $^{51}\text{V}^+$ -analysis. To calibrate vanadium concentrations for ICP-MS-measurements, we used certified CRM TORT-2 lobster hepatopancreas (1.64 ± 0.19 mg of vanadium per kg) and analytical vanadium standards.

From ICP-MS-measurements we obtained an average value of 166 ± 33 μg vanadium per kg of $V_{\text{Br}}\text{PO}(\text{AnI})$, leading to a ratio of 0.9 ± 0.2 of vanadium atoms per monomeric subunit on the basis of a bromoperoxidase concentration of 3.64 μM , and a molecular mass of the monomer of 60304 Da. The ratio of one vanadate cofactor per protein subunit agrees with results from X-ray diffraction analysis [19]. We therefore used the same ICP-MS-approach to determine the ratio of vanadate cofactor per protein subunit of the bromoperoxidase II, leading to a value of 0.5 ± 0.1 on the basis of a vanadium concentration of 60 ± 12 μg per kilogram of enzyme (ICP-MS), a bromoperoxidase II-concentration of 1.29 μM , and a molecular mass of 67439 per protein subunit.

3.1.3. Secondary structure

To model how the amino acid chain of vanadate-loaded bromoperoxidase II arranges to build a secondary structure in solution, we analyzed the circular dichroism (CD) associated with the carbonyl chromophore of the amide bond. The spectrum recorded for $V_{\text{Br}}\text{PO}(\text{AnII})$ between 184 and 260 nm shows positive Cotton-effects at 196 and 213 nm and negative Cotton-effects at 209 and 223 nm (pH 8.0, Tris/HCl-buffer; Fig. 4, red lane). The wavelength-dependence of the molar ellipticity $[\Theta]_m$ correlates in the applied numerical model [43–46] with a secondary structure of $V_{\text{Br}}\text{PO}(\text{AnII})$ composed of 52% helical domains, 5% β -sheets, 17% turns, and 27% random coils. The secondary structure of $V_{\text{Br}}\text{PO}(\text{AnI})$ (Fig. 4, black lane), in the same model, is built from 26% helical domains, 20% β -sheets, 22% turns, and 32% random coils. By this approach, the secondary structure of $V_{\text{Br}}\text{PO}(\text{AnII})$ shows more helical and less β -sheet domains than the bromoperoxidase I.

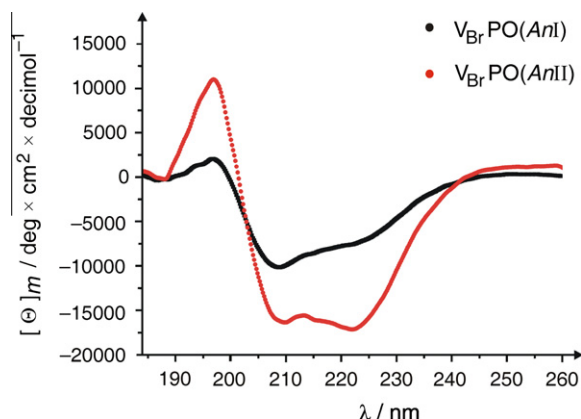


Fig. 4. CD-spectra of $V_{\text{Br}}\text{PO}(\text{AnII})$ and $V_{\text{Br}}\text{PO}(\text{AnI})$ (pH 8.0, H_2O , Tris/HCl buffer (1.27 μM for isoenzyme I and 0.25 μM for isoenzyme II, 20°C); $[\Theta]_m$ = molar ellipticity).

3.1.4. Tertiary and quaternary structure

On the basis of primary structure-homology (Fig. 2) and the known tertiary structure of $V_{\text{Br}}\text{PO}(\text{AnI})$ from X-ray diffraction analysis [19], we modeled a three-dimensional structure of the bromoperoxidase II (Fig. 5). In this solid state model, the ratio of α -helical domains (39%) versus β -sheets (9%) is similar to the $V_{\text{Br}}\text{PO}(\text{AnI})$ -tertiary structure in the crystal structure (41% helix, 6% β -sheet, and 51% random coil) [19]. The overall folding core of $V_{\text{Br}}\text{PO}(\text{AnI})$ thereby is predicted to be highly conserved in $V_{\text{Br}}\text{PO}(\text{AnII})$. The six cysteine residues known to form intramolecular disulfide bridges within the $V_{\text{Br}}\text{PO}(\text{AnI})$ -monomer [19] are present at similar positions in the $V_{\text{Br}}\text{PO}(\text{AnII})$ -protein (Fig. 2). Also, the two cysteine residues involved in dimer formation at the interface of $V_{\text{Br}}\text{PO}(\text{AnI})$ are conserved in $V_{\text{Br}}\text{PO}(\text{AnII})$ [Cys-3 and Cys-41, numbering in homology to $V_{\text{Br}}\text{PO}(\text{AnI})$ -numbering]. The vanadate cofactor in this model binds to the τ -imidazole-nitrogen of the histidine-517 side chain, leading to a distorted trigonal bipyramidal coordination sphere at vanadium. Close contacts thereby are possible between the apical vanadate oxygen and the τ -nitrogen of histidine-452, and between equatorially bound vanadate oxygens and the hydroxyl oxygen of serine-450, the ϵ -amino nitrogen of lysine-374, and one of the guanidinium nitrogens of arginine-382. The

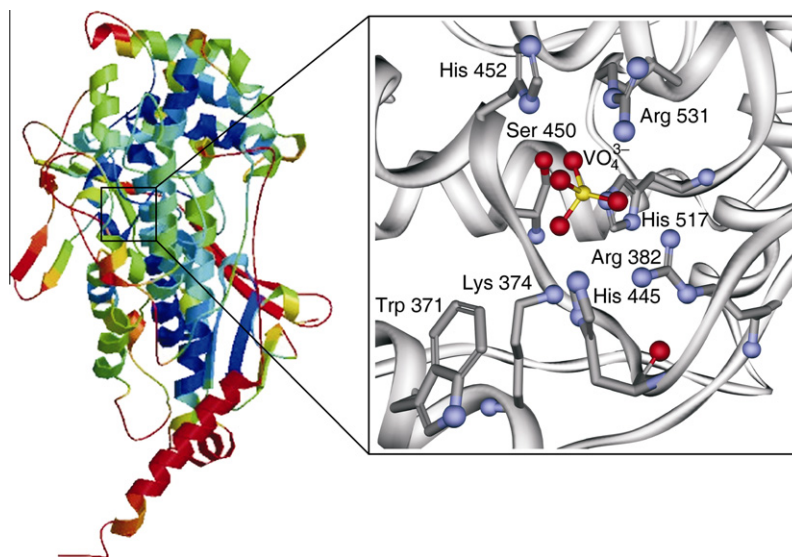


Fig. 5. Model of $V_{\text{Br}}\text{PO}(\text{AnII})$ -monomer based on sequence homology and the crystal structure of $V_{\text{Br}}\text{PO}(\text{AnI})$ [19]. The inaccuracy per residue was estimated and visualized using color gradient from blue (more reliable regions) to red (potentially unreliable regions). The region of the vanadate binding pocket was represented with the main residues (numbering of the mature 67.4-kDa protein) involved in vanadate coordination according to the $V_{\text{Br}}\text{PO}(\text{AnI})$ -structure [19].

amino-acids located in proximity to the active site of $V_{Br}PO(AnII)$, in this model, are similar to those found in the three-dimensional structure of $V_{Br}PO(AnI)$ (Fig. 5), being in line with homology from primary sequence alignment (Fig. 2). Since the two isoenzymes feature different vanadate reconstitution rates (Fig. 3), we think that additional structural aspects exist that control vanadate binding and bromoperoxidase activity, such as quaternary organization of monomers.

To address the aspect of quaternary organization and thus the issue of broken vanadate/monomer-ratio of active bromoperoxidase II, we performed gel filtrations using ferritin, bovine γ -globulin, conalbumin, ovalbumin, equine myoglobin, and vitamin B₁₂ as standards for a molecular mass-retention time correlation [$\lg(M_{\text{protein}}/\text{g mol}^{-1}) = -0.25 t/\text{min} + 8.46$; correlation coefficient $r = 0.9996$; Fig. 6] [47]. For calibrating the analytical method, we used $V_{Br}PO(AnI)$ as reference. A retention time of 13.47 min in this model correlates with a molecular mass of 136 kDa for $V_{Br}PO(AnI)$, which is 12% higher than the mass of 120 kDa determined via mass spectrometry and X-ray diffraction [19] of the homodimer. A retention time of 11.57 min, in this correlation, leads to a molecular mass of 420 kDa for $V_{Br}PO(AnII)$. From this number and the known mass of the monomeric unit, we concluded that $V_{Br}PO(AnII)$ is a hexamer.

Aggregation of monomeric subunits seems to be a common phenomenon for marine bromoperoxidases. In $V_{Br}PO(AnI)$, for example, two subunits form disulfide bridges, leading to a homodimer [19]. Twelve protein subunits aggregate to form the wild-type bromoperoxidase of the red alga *Corallina officinalis* [48]. Previous studies have shown that *L. digitata* $V_{Br}PO$ s are dimers that, in solution, spontaneously self-aggregate into higher molecular mass oligomers [49]. It is not known whether the close sequence homology between the $V_{Br}PO(AnII)$ - and $V_{Br}PO(Ldl)$ -proteins accounts for similar quaternary organization in solution.

The reason for bromoperoxidase monomers to form supramolecular entities is not known, and cooperative effects for substrate binding and thus rate effects on bromide oxidation have not yet been reported. From a chemical point of view, aggregation may be an evolutionary response to the fact that bromoperoxidases handle aggressive chemicals, such as hydrogen peroxide and reactive bromoelectrophiles (vide infra). Both reactants have the potential to irreversibly transform an active bromoperoxidase site in such a way that the enzyme loses its bromide oxidation ability [50]. If one subunit became inactive, the remaining subunit(s) would retain bromoperoxidase activity to continue bromide oxidation. This interpretation implies that bromide oxidation is vital for the producing organism.

3.2. Reactivity of the bromoperoxidase II

Based on structural differences we expected different chemical reactivity of bromoperoxidases I and II from *A. nodosum* and there-

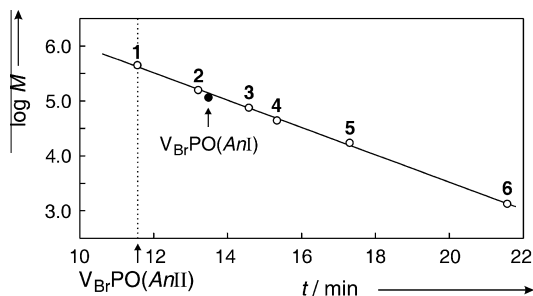
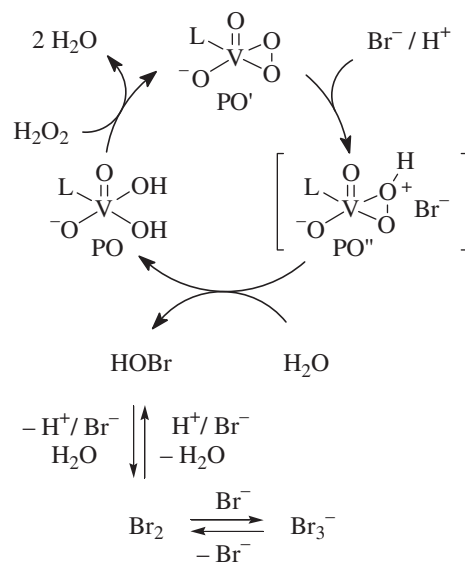


Fig. 6. Determination of molecular mass of $V_{Br}PO(AnII)$ (...) via gel filtration [1, ferritin (440 kDa); 2, bovine γ -globulin (158 kDa); 3, conalbumin (75 kDa); 4, ovalbumin (43 kDa); 5, equine myoglobin (17 kDa); 6, vitamin B₁₂ (1.4 kDa)].



Scheme 1. Model for interpretation of steady-state kinetic data for $V_{Br}PO(AnII)$ -catalyzed bromide oxidation by hydrogen peroxide [bi-bi-ping-pong mechanism; $PO = V_{Br}PO(AnII)$; PO' and PO'' = loaded derivatives of PO ; $K_m^{H_2O_2}$ and $K_m^{Br^-}$ refer to Michaelis–Menten parameters for substrates H_2O_2 and Br^- , and $K_i^{Br^-}$ for competitive enzyme inhibition by bromide].

fore investigated the mechanism of bromide oxidation (Section 3.2.1), chemical properties of bromination reagent relevant for carbon-bromine bond formation (3.2.2), and explored biometric synthesis of a marine natural product (3.2.3).

According to the general mechanism (cf. Scheme 1), bromoperoxidases catalyze oxidation of bromide by hydrogen peroxide and release a bromoelectrophile to bromofunctionalize an organic substrate in a non enzymatic process. To probe the chemical nature of the bromoelectrophile that is responsible for selectivity in carbon-bromine bond formation in bulk solution, we investigated phenol bromination via competition kinetics. It is not yet known, whether phenols are endogenous substrates for bromoperoxidases.

3.2.1. Steady-state kinetics

We investigated the mechanism of enzymatic bromide oxidation via steady-state kinetics, performed under substrate saturation conditions (Scheme 1, Table 1). The hydrogen peroxide concentration thereby was gradually raised from 0.02 mM to 1.00 mM, at fixed bromide concentration between 1.00 mM and 400 mM. The ionic strength of the solutions was adjusted with sodium sulfate to 0.8 M, which is similar to the ionic strength of ocean water (0.55–0.70 M) and allows to compare kinetic data for bromide oxidation catalyzed by $V_{Br}PO(AnII)$ to those of other vanadate(V)-dependent bromoperoxidases [14]. The analytical method to measure rates under saturation conditions is the monochlorodimedone (MCD) assay.

For numerical analysis of steady-state kinetic data, we used the bi-bi-ping-pong-reaction model [Scheme 1, Eqs. (1)–(4)] [51–53]. According to this mechanistic scheme, $V_{Br}PO(AnII)$ (in short: PO) and one of the substrates provide in a bimolecular reversible reaction intermediate PO' . In the second step, the substrate having less affinity for binding to PO reversibly reacts in a bimolecular reaction with PO' to give PO'' . PO'' hydrolyzes in a non rate-determining step to furnish the product of bromide oxidation and the resting state of the enzyme, that is, PO . Binding of bromide to PO furnishes competitively inhibited enzyme PO''' . Nothing is known so far about the mode of bromide binding to the active site [54], but the equilibrium constant for this associative process is available from the steady state kinetics.

Table 1
Steady-state kinetic parameters of $V_{Br}PO(AnII)$ (22 ± 0.5)^a.

Entry	pH	V_{max}/U^b (mg^{-1})	k_{cat} (s^{-1})	$K_m^{Br^-}$ (mM)	$K_m^{H_2O_2}$ (μM)	$K_i^{Br^-}$ ^c (mM)
1	5.9 ^d	68 ± 4	153	0.32 ± 0.11	22.5 ± 3.6	125
2	7.2 ^e	22 ± 1	49	1.22 ± 0.14	7.8 ± 0.8	4242

^a Ionic strength adjusted with sodium sulfate to 0.8 M; $87 \pm 4 U^0_{MCD} mg^{-1}$; data for $V_{Br}PO(AnI)$: $k_{cat} = 85 s^{-1}$; $K_m^{Br^-} = 3.71 \pm 0.26$ mM; $K_m^{H_2O_2} = 55.0 \pm 6.0 \mu M$; all values for pH 5.9, $I = 0.8$ M [14,55].

^b Determined with the MCD-assay (Supplementary material).

^c The experimental error for $K_i^{Br^-}$ is ± 30 –60%.

^d MES-buffer.

^e HEPES-buffer.

From hydrogen peroxide- and bromide-concentration dependence of rates of enzymatic bromide oxidation [$v_{oxidation}$, Eq. (5)], we calculated the maximum velocity of the reaction (V_{max}), Michaelis parameters associated with the two reversible steps ($K_m^{H_2O_2}$, $K_m^{Br^-}$), and the constant $K_i^{Br^-}$ describing competitive enzyme inhibition by bromide (Table 1). The quality of the fits, as expressed by the magnitude of correlation coefficients, is similar to the correlation of data from steady-state kinetics obtained for isoenzyme I [14]. We therefore concluded that bromide oxidation catalyzed by $V_{Br}PO(AnII)$ and $V_{Br}PO(AnI)$ follows the same mechanism (Scheme 1).



$$v_{oxidation} = \frac{v_{max} [H_2O_2]}{\left(1 + \frac{K_m^{Br^-}}{[Br^-]}\right) \left(1 + \frac{K_m^{H_2O_2}}{[H_2O_2]}\right) + [H_2O_2]} + \frac{K_m^{H_2O_2}}{K_m^{Br^-}} \frac{\left(1 + \frac{K_m^{Br^-}}{[Br^-]}\right)}{\left(1 + \frac{K_m^{H_2O_2}}{[H_2O_2]}\right)} [H_2O_2] \quad (5)$$

The experimental data show that bromoperoxidase II-reactivity increases by a factor three as pH of the solution changes from 7.2 to 5.9. $V_{Br}PO(AnII)$ binds under both conditions bromide and hydrogen peroxide notably stronger than isoenzyme I (Table 1, footnote a). From absolute values of $K_m^{H_2O_2}$ and $K_m^{Br^-}$ we concluded that hydrogen peroxide is the first of the substrates to bind to the vanadate active site, leading to enzyme-bound peroxidovanadate(V). The affinity for hydrogen peroxide addition thereby grows as the reaction mixture becomes less acidic, which is in line with the nucleophilic behavior of the peroxide in the addition to vanadate(V). Bromide also is a nucleophile, but its affinity to approach the peroxido-loaded active site in the second step decreases as the pH rises from 5.9 to 7.2, possibly for reasons of electron pair repulsion as protons at the active site become less available for hydrogen bonding. At elevated concentration, bromide reversibly inhibits the enzymatic oxidation (vide supra). From the magnitude of $K_i^{Br^-}$ we concluded that bromide concentration for synthetic application should remain below 0.1 M, to minimize this rate retarding effect.

3.2.2. The bromination reagent – a linear free energy relationship

The chemical nature of the bromination reagent obtained from $V_{Br}PO(AnII)$ -catalyzed bromide oxidation by hydrogen peroxide, relevant for explaining reactivity in arene bromination was characterized in a competition kinetic study. The approach to identify the nature of an intermediate in physical organic chemistry is correla-

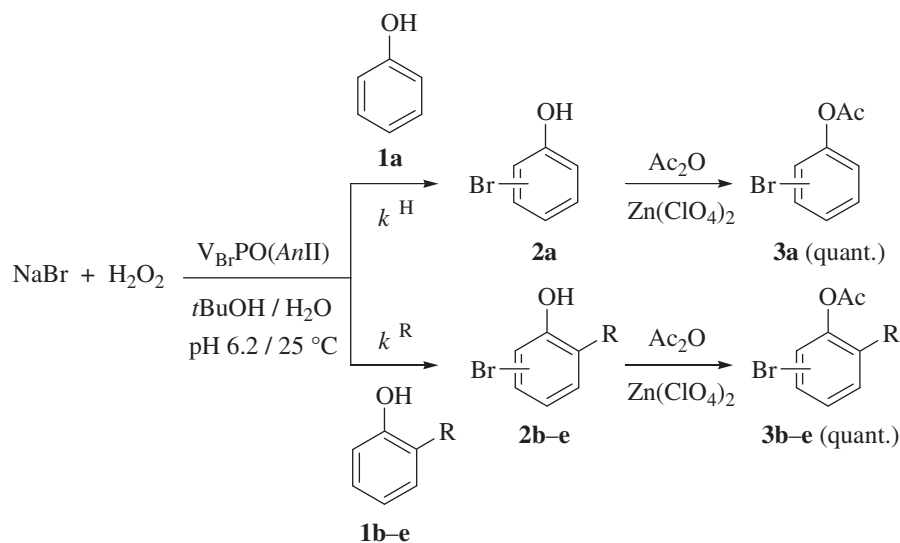
tion analysis [56,57]. In correlation analysis, according to Hammett, Hansch, Leo, and Taft, polar effects of substituents on rates in a series of homologous reactions are quantitatively described by substituent constants, such as σ_m [Eq. (6)]. A σ_m -constant reflects the sum of inductive and mesomeric effects of a substituent R on the rate of a reference reaction. The polar effect of R in this series is compared to the hydrogen atom (R = H). A plot of relative rate constants, as expressed in $\log k^R/k^H$ versus σ_m ($\sigma_m = 0$ for H), provides from the slope of a linear correlation a reaction parameter ρ (Eq. (6)). Sign and magnitude of the reaction parameter characterize responsiveness of the substrate toward polar effects, exerted by the reactive intermediate.

$$\log \frac{k^R}{k^H} = \rho \cdot \sigma_m \quad (6)$$

For measuring relative rates of hydrocarbon bromination in $V_{Br}PO(AnII)$ -catalyzed reactions, we devised a competition system, based on bromination of phenol (**1a**) as reference, and derivatives **1b–e** as reporter substrates (Scheme 2). Due to difficulties in reliably quantifying yields of phenols via GC, we converted bromophenol mixtures (products **2a–e**), obtained from competition kinetics, into *O*-acetyl derivatives **3a–e**, to determine product ratios and thus relative rate constants according to Eq. (7) (Scheme 2, Table 2).

In controls and in competition experiments, bromination of phenols **1a–e** occurs in *ortho*- and in *para*-position with respect to the hydroxyl substituent. The ratio of *ortho*-substitution increases along the series of substituents R = CH₃ (*ortho:para* = 21:79) via H, C(CH₃)₃, OCH₃ to Cl (50:50) (Supplementary Material). Since *ortho*-substitution adds a steric component to chemical reactivity that is not covered by σ_m , we, like others, used the values from *para*-substitution for calculating relative rate constants of phenol bromination [58,59].

A plot of $\log(k_p^R/k_p^H)$ -values versus substituent parameters σ_m provides $\rho = -2.5$ from the slope of a linear correlation (Fig. 7). The negative sign of the reaction parameter ρ points to an electrophilic behavior of the effective bromination reagent [58,59]. To compare the ρ -value from the enzymatic reaction to reagents that generally are put forward to explain reactivity in bromoperoxidase chemistry, such as hypobromous acid, molecular bromine, and tribromide, we performed controls. Hypobromous acid thereby is not able to brominate phenol **1a** at pH 6.2. Competition kinetics on phenol bromination by molecular bromine, furnish under otherwise identical conditions a reaction parameter of $\rho = -1.9$ (Supplementary Material). Caesium tribromide and tetrabutylammonium tribromide, the reagents intended to be used for conducting competition kinetics similar to the procedure outlined for $V_{Br}PO(AnII)$ -catalyzed oxidations are sparingly soluble in aqueous *tert*-butanol, and thus prevented us from performing correlation analysis for tribromide-mediated phenol bromination. The tribromide anion, on the other hand, is a nucleophile, which has to dissociate into bromide (nucleophilic) and bromine (electrophilic) to be effective in electrophilic aromatic substitution. Bromine liber-



$$\frac{[\mathbf{1b-e}]}{[\mathbf{1a}]} = \frac{k^R}{k^H} \frac{[\mathbf{3b-e}]}{[\mathbf{3a}]} \quad (\text{eq. 7})$$

Scheme 2. Reaction scheme for kinetic experiments in the phenol-competition system [for data analysis, see eqs. 6–7; index for compounds **1** and **2**: R = H for **a**, CH₃ for **b**, C(CH₃)₃ for **c**, OCH₃ for **d**, and Cl for **e**].

ated from tribromide, in turn, is expected to show reactivity similar to molecular bromine outlined above [60].

The close analogy of relative rate constants and parameter ρ for phenol bromination in bromoperoxidase II-catalyzed oxidation and by molecular bromine led us to the conclusion that the reactivity determining reagent in both instances is the same. Since all experimental details in this study are explicable by the chemistry of molecular bromine, we propose that bromine is the bromoelectrophile, which transforms in bromoperoxidase-catalyzed oxidations phenols (e.g. **1**), and possibly other π -nucleophiles, into bromoderivatives (e.g. **2**). Alternatives, such as hypobromous acid or the tribromide-anion, are expected to coexist with bromine in solutions obtained from bromoperoxidase-catalyzed oxidation, without being directly involved in carbon-bromine bond formation. However, we wish to point out that some selectivities, such as *ortho/para*-ratios and the noteworthy propensity of **1a** to furnish the product of monobromination in the enzymatic reaction, differ from controls performed with molecular bromine, suggesting possible selectivity effects imposed by the bromoperoxidase protein.

Table 2
Relative rate constants of phenol bromination in bromoperoxidase-catalyzed oxidations and substituent parameters σ_m ^a used for correlation analysis.

Entry	R	1	σ_m	k_p^R/k_p^H ^b
1	H	a	0.00	–
2	CH ₃	b	–0.11	1.70
3	C(CH ₃) ₃	c	–0.02	0.71
4	OCH ₃	d	0.05	0.63
5	Cl	e	0.31	0.13

^a σ_m refers to substituent constants for correlation analysis, derived from ¹⁹F-NMR spectroscopy for analyzing, for example, polar substituent effects in aromatic substitution

^b $p(\text{ara})$ with respect to the hydroxyl group in **1**.

3.2.3. Biomimetic synthesis

As example for biomimetic synthesis of a naturally occurring organobromine via V_{Br}PO(AnII)-catalyzed oxidation, we explored synthesis of methyl 4-bromopyrrole-2-carboxylate (**Scheme 3**), a compound that was isolated from the marine sponge *A. tenuidigitata*. We adapted for the synthetic part conditions regarding solvent, buffer capacity, mode of hydrogen peroxide administration, and specific enzymatic activity, that we had developed in an earlier study for pyrrole bromination in bromoperoxidase I-catalyzed oxidation [14]. Under such conditions, pyrrole **4** underwent in a reproducible manner about 35% conversion, to furnish a 71/29-mixture of bromopyrroles **5a** and **5b** in a total yield of 31% (**Scheme 3**).

4. Conclusion

The vanadate(V)-dependent bromoperoxidases I and II isolated from *A. nodosum* differ in structure and reactivity. The bromoperoxidase II, thereby is the larger, structurally more complex, more

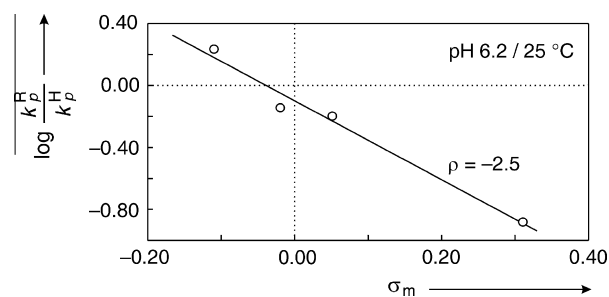
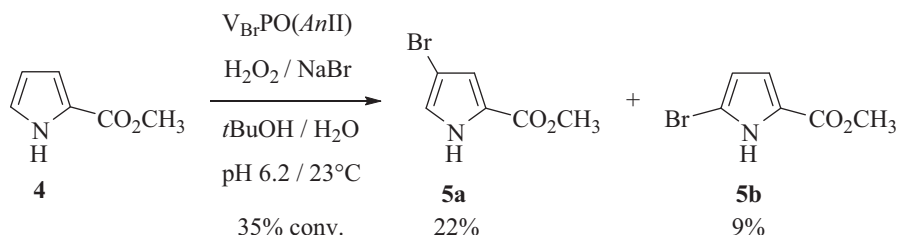


Fig. 7. Correlation of $\log(k_p^R/k_p^H)$ versus σ_m according to eq. 6 for oxidative phenol bromination in V_{Br}PO(AnII)-catalyzed reactions [$\log(k_p^R/k_p^H) = -2.5\sigma_m - 0.10$ ($r = 0.990$) for substitution in *para*-position to the hydroxyl group in **1**].



Scheme 3. Bromination of methyl pyrrole-2-carboxylate in bromoperoxidase II-catalyzed oxidation [conditions: 63 $\mu\text{mol}\%$ of $\text{V}_{\text{Br}}\text{PO}(\text{AnII})$ (34.6 U_T), 2.2 equiv. of NaBr, and 2.2 equiv. of H_2O_2].

reactive, but chemically under turnover conditions also less stable enzyme. From correlation analysis and independent controls we concluded that the product of enzymatic bromide oxidation responsible for describing reactivity and selectivity in arene bromination is molecular bromine.

Bromine in a solution of aqueous *tert*-butanol is able to convert phenols and methyl pyrrole-2-carboxylate at pH 6.2 into bromoderivatives. The latter reaction, in our opinion, not only is of interest for stimulating discussion on biosynthesis of pyrrole-derived bromometabolites in nature, but also raises the question about further functional groups that are receptive for bromofunctionalization in $\text{V}_{\text{Br}}\text{PO}$ -catalyzed oxidations, to obtain a deeper insight into significance role of bromoperoxidases for synthesis of naturally occurring organobromines. A correlation of this kind is under current investigation in our laboratories.

As concluding remark we wish to address a question raised by early contributions to this field of research, that is the classification of bromoperoxidases I and II from *A. nodosum* as glycoproteins [34]. Although we observed chemical transformation upon treatment of the two bromoperoxidases with PNGase, we could not relate these findings to hydrolysis of carbohydrate subunits from the proteins. From crystal structure analysis it is meanwhile clear that $\text{V}_{\text{Br}}\text{PO}(\text{AnI})$ is no glycoprotein [19]. A similar approach probably has to be pursued for finally settling this debate also for $\text{V}_{\text{Br}}\text{PO}(\text{AnII})$.

Acknowledgments

This work is dedicated to Professor Dr. Dr. h.c. Gerhard Bringmann, on the occasion of his 60th birthday. We thank Prof. Dr. Rita Bernhardt, Dipl.-Biol. Kerstin Ewen, and Dr. Frank Hannemann for technical advice in recording CD-spectra, Dr. Jean-Pierre Stockis and Dipl.-Math. Marion Weber for helpful discussion on numerical data analysis, and Ms. Astrid Hoppe for technical assistance in experiments associated with reconstitution of apobromoperoxidases. This work is part of the Ph.D. thesis of D.W. and the diploma work of M.R.

Appendix A. Supplementary material

Supplementary data associated with this article can be found, in the online version, at <http://dx.doi.org/10.1016/j.bioorg.2012.05.003>.

References

- [1] G. Müller, G. Knusi, H.F. Schöler, J. Prakt. Chem. 338 (1996) 23–29.
- [2] C.J. Cooksey, Molecules 6 (2001) 736–769.
- [3] P. Friedländer, Ber. Dtsch. Chem. Ges. 42 (1909) 765–770.
- [4] J.-M. Kornprobst, Encyclopedia of Marine Natural Products, vol. 1, Wiley-VCH, Weinheim, 2010, pp. 251–422.
- [5] C. Leblanc, C. Colin, A. Cosse, L. Delage, S. La Barre, P. Morin, B. Fiévet, C. Voiseux, Y. Ambroise, E. Verhaeghe, D. Amouroux, O. Donard, E. Tessier, P. Potin, Biochimie 88 (2006) 1773–1785.
- [6] G.W. Gribble, Environ. Sci. Pollut. Res. 7 (2000) 37–47.
- [7] S.L. Neidleman, J. Geigert, Biohalogenation, Principles, Basic Roles and Application, Ellis Horwood, Chichester, 1986.
- [8] R. Frim, S.D. Ukeles, Bromine, in: Industrial Minerals & Rocks, J.E. Kogel, N.C. Trivedi, J.M. Baker (Eds.), Society for Mining, Metallurgy, and Exploration, 7th ed., Littleton, Colorado, 2006, pp. 285–294.
- [9] J. Hartung, Angew. Chem., Int. Ed. Engl. 38 (1999) 1209–1211.
- [10] J. Hartung, Y. Dumont, M. Greb, D. Hach, F. Köhler, H. Schulz, M. Časny, D. Rehder, H. Vilter, Pure Appl. Chem. 81 (2009) 1251–1264.
- [11] A. Butler, Coord. Chem. Rev. 187 (2009) 17–35.
- [12] J.W. Blunt, B.R. Copp, W.-P. Hu, M.H.G. Munro, P.T. Northcote, M.R. Prinsep, Nat. Prod. Rep. 28 (2011) 196–268.
- [13] H.S. Soedjak, A. Butler, Biochim. Biophys. Acta 1079 (1991) 1–7.
- [14] D. Wischang, J. Hartung, Tetrahedron 67 (2011) 4048–4054.
- [15] A. Butler, J.V. Walker, Chem. Rev. 93 (1993) 1937–1944.
- [16] H. Vilter, Vanadate-Dependent Haloperoxidases, in: Metal Ions in Biological Systems, H. Sigel, A. Sigel (Eds.), Vanadium and its role in life, vol. 31, Dekker, New York, 1995, pp. 325–362.
- [17] For a review on biohalogenation: F.H. Vaillancourt, E. Yeh, D.A. Vosburg, S. Garneau-Tsodikova, C.T. Walsh, Chem. Rev. 106 (2006) 3364–3378.
- [18] For Database Dealing with Information on Bromoperoxidases, <http://www.brenda-enzymes.info/php/result_flat.php4?ecno=1.11.1.18&organism=>>.
- [19] M. Weyand, H.-J. Hecht, M. Kieß, M.-F. Liand, H. Vilter, D. Schomburg, J. Mol. Biol. 293 (1999) 595–611.
- [20] D. Wischang, O. Brücher, J. Hartung, Coord. Chem. Rev. 255 (2011) 2204–2217.
- [21] A. Butler, M. Sandy, Nature 460 (2009) 848–854.
- [22] H. Vilter, Phytochemistry 23 (1984) 1387–1390.
- [23] H. Vilter, K.-W. Glombitza, A. Grawe, Bot. Mar. 26 (1983) 331–340.
- [24] C. van den Hoek, H.M. Jahns, D.G. Mann, Algen, 3rd ed., Thieme, Stuttgart, 1993, pp. 132–166.
- [25] H. Vilter, Methods Enzymol. 228 (1994) 665–672.
- [26] J. Hartung, O. Brücher, D. Hach, H. Schulz, H. Vilter, G. Ruick, Phytochemistry 69 (2008) 2826–2830.
- [27] M.G.M. Tromp, G. 'Olafsson, B.E. Krenn, R. Wever, Biophys. Biochim. Acta 1040 (1990) 192–198.
- [28] E. de Boer, R. Wever, J. Biol. Chem. 263 (1988) 12326–12332.
- [29] A. Butler, A.H. Baldwin, Struct. Bond. 89 (1997) 109–132.
- [30] J.V. Walker, A. Butler, Inorg. Chim. Acta 243 (1996) 201–206.
- [31] D. Wischang, J. Hartung, T. Hahn, R. Ulber, T. Stumpf, C. Fecher-Trost, Green Chem. 13 (2011) 102–108.
- [32] R.R. Everett, J.R. Kanofsky, A. Butler, J. Biol. Chem. 265 (1990) 4908–4914.
- [33] B.E. Krenn, H. Plat, M.G.M. Tromp, H. Vilter, R. Wever, Abstracts of the 14th International Congress of Biochemistry, vol. 4, Czechoslovakia, Prague, 1988, pp. 103.
- [34] B.E. Krenn, M.G.M. Tromp, R. Wever, J. Biol. Chem. 264 (1989) 19287–19292.
- [35] N.S. Reddy, P. Ramesh, T.P. Rao, Y. Venkateswarlu, Indian J. Chem. B38 (1999) 1145–1147.
- [36] K.E. Apt, S.K. Clendennen, D.A. Powers, A.R. Grossman, Mol. Gen. Genet. 246 (1995) 455–464.
- [37] E. Scotto-Lavino, G. Du, M.A. Frohman, Nat. Protocol 1 (2006) 2742–2745.
- [38] L.P. Hager, D.R. Morris, F.S. Brown, H. Eberwein, J. Biol. Chem. 241 (1966) 1769–1777.
- [39] F. Björkstén, Eur. J. Biochem. 5 (1968) 133–142.
- [40] E. Verhaeghe, D. Buisson, E. Zekri, C. Leblanc, P. Potin, Y. Ambroise, Anal. Biochem. 379 (2008) 60–65.
- [41] C. Wagner, I.M. Molitor, G.M. König, Phytochemistry 69 (2008) 323–332.
- [42] W.D. Hewson, L.P. Hager, J. Phycol. 16 (1980) 340–345.
- [43] L. Whitmore, B.A. Wallace, Biopolymers 89 (2007) 392–400.
- [44] N.J. Greenfield, G.D. Fasman, Biochemistry 8 (1969) 4108–4116.
- [45] N.J. Greenfield, Anal. Biochem. 235 (1996) 1–10.
- [46] CDPro programs for CD analysis SELCON3, CDSSTR and CONTINLL. CDPro package: N. Sreerama, R.W. Woody, Anal. Biochem. 287 (2000) 252–260; SELCON3: N. Sreerama, S.Y.U. Venyaminov, Protein Science 8 (1999) 370–380; CDSSTR: W.C. Johnson, Proteins: Str. Func. Genet. 35 (1999) 307–312; CONTINLL: S.W. Provencher, J. Gloeckner, Biochemistry 20 (1981) 33–37.
- [47] E. Stellwagen, Methods Enzymol. 182 (1990) 317–328.
- [48] M.N. Isupov, A.R. Dalby, A.A. Brindley, Y. Izumi, T. Tanabe, G.N. Murshudov, J.A. Littlechild, J. Mol. Biol. 299 (2000) 1035–1049.
- [49] C. Colin, C. Leblanc, E. Wagner, L. Delage, E. Leize-Wagner, A. Van Dorsselaer, B. Kloareg, P. Potin, J. Biol. Chem. 278 (2003) 23545–23552.
- [50] G.F.M. Winter, A. Butler, Biochemistry 35 (1996) 11805–11811.
- [51] H.J. Fromm, Initial Rate Enzyme Kinetics, Springer-Verlag, Berlin (West), New York, 1975.

- [52] C.-R. Yang, B.E. Shapiro, E.D. Mjolsness, G.W. Hatfield, *Bioinformatics* 21 (2005) 774–780.
- [53] W.W. Cleland, *Biochim. Biophys. Acta* 67 (1963) 104–137.
- [54] H. Dau, J. Dittmer, M. Epple, J. Hanss, E. Kiss, D. Rehder, C. Schulzke, H. Vilter, *FEBS. Lett.* 457 (1999) 237–240.
- [55] Michealis-Menten parameter for isoenzyme I refer to MES-buffered solutions. By mistake in Ref. [14] we described the buffer in the text as phosphate buffer (pH 5.9) although in the experimental the buffer is correctly described as MES.
- [56] A. Williams, *Free energy Relationships in Organic and Bio-organic Chemistry*, Royal Chemical Society, Cambridge, 2003 (Chapters 1 and 2).
- [57] C. Hansch, A. Leo, R.W. Taft, *Chem. Rev.* 91 (1991) 165–195.
- [58] O.S. Tee, M. Paventi, J.M. Bennett, *J. Am. Chem. Soc.* 111 (1989) 2233–2240.
- [59] G. Guo, F. Lin, *J. Hazard. Mater.* 170 (2009) 645–651.
- [60] E. Berliner, M.C. Beckett, *J. Am. Chem. Soc.* 79 (1957) 1425–1431.